Cutoff-Free Circuit Quantum Electrodynamics

Moein Malekakhlagh, Alexandru Petrescu, and Hakan E. Türeci

Phys. Rev. Lett. **119**, 073601 — Published 16 August 2017

DOI: 10.1103/PhysRevLett.119.073601

Cutoff-free Circuit Quantum Electrodynamics

Moein Malekakhlagh, Alexandru Petrescu, and Hakan E. Türeci
Department of Electrical Engineering, Princeton University, Princeton, New Jersey, 08544
(Dated: July 18, 2017)

Any quantum-confined electronic system coupled to the electromagnetic continuum is subject to radiative decay and renormalization of its energy levels. When coupled to a cavity, these quantities can be strongly modified with respect to their values in vacuum. Generally, this modification can be accurately captured by including only the closest resonant mode of the cavity. In the circuit quantum electrodynamics architecture, it is however found that the radiative decay rates are strongly influenced by far off-resonant modes. A multimode calculation accounting for the infinite set of cavity modes leads to divergences unless a cutoff is imposed. It has so far not been identified what the source of divergence is. We show here that unless gauge invariance is respected, any attempt at the calculation of circuit QED quantities is bound to diverge. We then present a theoretical approach to the calculation of a finite spontaneous emission rate and the Lamb shift that is free of cutoff.

Introduction. An atom-like degree of freedom coupled to continuum of electromagnetic (EM) modes spontaneously decays. When the atom is confined in a resonator, the emission rate can be modified compared with its value in free space, depending on the EM local density of states at the atomic position [1–4], which is called the Purcell effect [5]. An accompanying effect is the Lamb shift, a radiative level shift first observed in the microwave spectroscopy of the hydrogen $^2P_{1/2} - {}^2S_{1/2}$ transition [6]. These quantities have been experimentally accurately characterized for superconducting Josephson junction (JJ) based qubits coupled to coplanar transmission lines [7, 8] and three-dimensional resonators [9]. In the dispersive regime where a qubit with transition frequency ω_j is far-detuned from the nearest resonant cavity mode (frequency ν_r, loss κ_r), single mode expressions exist for the Purcell decay rate, $\gamma_P = (g/\delta)^2\kappa_r$ and the Lamb shift, $\Delta_L = g^2/\delta$. These well-known approximate estimates are often used in analyzing qubit state readout, hence we employ them to benchmark our results. Here g denotes the coupling between the qubit and the cavity mode and $\delta = \omega_j - \nu_r$ denotes their detuning [10]. However, for large couplings accessible in circuit QED, the single mode approximation is often inaccurate [7, 8]. In addition, due to particular boundary conditions imposed by the capacitive coupling of a resonator to external waveguides, the qubit relaxation time is limited by the EM modes that are far-detuned from the qubit frequency [8]. Similarly the measured Lamb shift in the dispersive regime can only be accurately fit with an extended Jaynes-Cummings (JC) model including several modes and qubit levels [7]. The Purcell rate has been generalized to account for all modes

$$\gamma_P = \sum_n (g_n/\delta_n)^2\,\kappa_n, \tag{1}$$

where g_n and $\delta_n = \omega_j - \nu_n$ are coupling to and detuning from resonator mode n with frequency ν_n and decay rate κ_n. Expression (1) is divergent without imposing a high-frequency cutoff [8]. Divergences appear as well in the Lamb shift and other vacuum-induced phenomena, e.g. photon-mediated qubit-qubit interactions [11]. These divergences are neither specific to the dispersive limit nor to the calculational scheme used to compute QED quantities. This issue is well-known for the Lamb shift [6], but less noted for the spontaneous emission rate. Indeed, free space spontaneous emission rate diverges as well, as we show in [12]. The finite result by Wigner and Weisskopf [13, 14] is due to Markov approximation which filters out the ultraviolet divergence. Recent generalizations of the Wigner-Weisskopf approach imposes an artificial cut-off to obtain a finite result [15]. So far, no satisfactory theoretical explanation has been given for these divergences. Here we address this issue within the framework of circuit quantum electrodynamics [16] (QED) and show that finite expressions can be obtained when gauge invariance is respected. We focus here on a superconducting artificial atom coupled to an open transmission-line resonator, but our results should be valid for other types of one-dimensional open EM environments as well.

Gauge invariance in circuit QED. The role of gauge invariance in accounting for light-matter interaction has been a vexing question since the beginnings of QED (see Ref. [17], and references therein). Hence, we first discuss gauge invariance in superconducting electrical circuits, and its impact on QED observables.

We consider a weakly nonlinear charge qubit (e.g. transmon [18][19]) capacitively coupled to a transmission-line resonator that in turn is coupled at both ends to semi-infinite waveguides (Fig. 1a). We assign flux variables to nodes, $\Phi_n(t) = \int^t d\tau\, V_n(\tau)$, with $V_n(t)$ being the instantaneous voltage at node n with respect to the ground node [16, 20]. Fixing the ground amounts to a particular gauge choice [16]. For the connection geometry in Fig 1a, the light-matter interaction derives from the energy on the coupling capacitor in the dipole approximation, $T_{\text{int}} = \frac{1}{2}C_g[\dot{\Phi}(x_0) - \dot{\Phi}_j]^2$ [12], with x_0 the qubit position. If from the three terms in its expansion, $T_{\text{EM}} = \frac{1}{2}C_g\dot{\Phi}(x_0)^2$, $T_{\text{EM-JJ}} = -C_g\dot{\Phi}(x_0)\cdot\dot{\Phi}_j$ and $T_{\text{JJ}} = \frac{1}{2}C_g\dot{\Phi}_j^2$, only the direct interaction $T_{\text{EM-JJ}}$ is kept, a multimode JC model in terms of circuit parameters can be derived [21], but gives rise to a diverging Purcell rate using Eq. (1). This open JC Model involves a two level approximation (TLA) of the JJ Hilbert space, the ro-

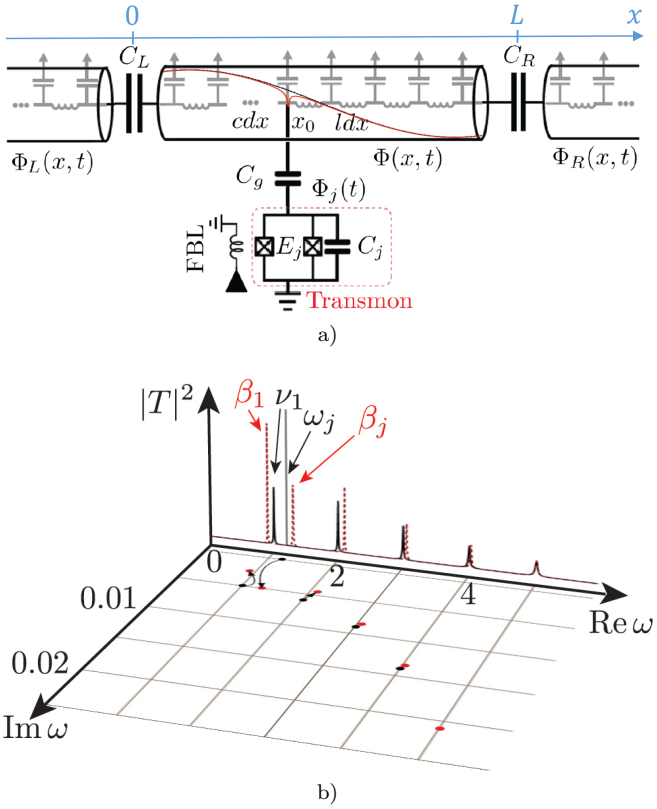

FIG. 1. a) A transmon qubit coupled to an open superconducting resonator. The black dashed line is a cartoon of the fundamental bare mode of the resonator, while the red solid curve represents the modified resonator mode. b) The transmission $|T|^2$ is shown versus the real frequency for the bare resonator modes (solid black curves). Capacitively coupling the qubit, whose transition frequency ω_j is slightly above the fundamental resonator frequency ν_1, gives rise to hybridized modes (dashed red curves). Alternatively, one may study the positions of these resonances in the complex frequency plane, where the bare resonator and qubit poles (black points) are displaced into hybridized resonator-like and qubit-like resonances (red points). The Purcell decay and the Lamb shift are obtained as the displacement of the qubit-like pole. The bare (hybridized) complex frequencies are the poles (zeros) of the characteristic function $D_j(s)$.

tating wave approximation (RWA) to drop nonresonant contributions, and the Born and Markov approximations leading to a Master equation accounting for losses due to resonator-waveguide coupling. It is unclear which approximation underlies the divergence, or whether the divergence can be resolved within the effective subgap circuit QED field theory.

We first note that keeping only the direct interaction $T_{\text{EM-JJ}}$ violates gauge invariance. We find that inclusion of all terms, in particular T_{EM}, equivalent to the diamagnetic A^2 term in the minimal coupling Hamiltonian $(p-eA)^2/2m$ [22], is essential to make all studied QED observables finite.

The A^2-term is thought to have no impact on transition frequencies in vacuum-induced effects such as the Lamb shift. Because it does not involve atomic operators, it is expected to make the same perturbative contribution to every atomic energy level, precluding observable shifts in *transition* frequencies [23]. This argument relies on perturbation theory in the A^2-term. We show that the diamagnetic term *does* have an impact when accounted for exactly to all orders.

Heisenberg equations of motion describing the infinite network in Fig. 1a, extending from $x=-\infty$ to $x=\infty$, are [12, 24]

$$\hat{\ddot{\varphi}}_j(t)+(1-\gamma)\omega_j^2\sin\left[\hat{\varphi}_j(t)\right]=\gamma\partial_t^2\hat{\varphi}(x_0,t), \tag{2}$$

$$\left[\partial_x^2-\chi(x,x_0)\partial_t^2\right]\hat{\varphi}(x,t)=\chi_s\omega_j^2\sin\left[\hat{\varphi}_j(t)\right]\delta(x-x_0) \tag{3}$$

Here $\hat{\varphi}_j(t)$ and $\hat{\varphi}(x,t)$ are dimensionless flux operators for the JJ and the resonator-waveguide system, respectively, $\gamma\equiv C_g/(C_g+C_j)$ is a capacitive ratio, $\chi_s=\gamma C_j/cL$ is the dimensionless series capacitance of C_g and C_j, ω_j is the dimensionless transmon frequency, and $\chi_i\equiv C_i/(cL)$ for $i=g,j,R,L$ [12]. These two inhomogeneous equations show that the flux field at x_0 drives the dynamics of the JJ [Eq. (2)], while the JJ acts as a source driving the EM fields [Eq. (3)]. In addition, the fields are subject to continuity conditions at the ends of the resonator $x=0,1$ (in units of L).

It is instructive to trace the individual terms of T_{int} in Eq. (2). T_{JJ} modifies the qubit frequency, renormalizing γ from C_g/C_j to $C_g/(C_g+C_j)$, while the direct interaction term $T_{\text{EM-JJ}}$ gives source terms in both equations. Most importantly, T_{EM} introduces an effective scattering term in the wave equation describing the fields in the transmission line, by modifying the unitless capacitance per length from 1 to $\chi(x,x_0)=1+\chi_s\delta(x-x_0)$. Consequently, these equations are consistent [22] with Kirchhoff's law of current conservation. In particular, at $x=x_0$, Eq. (2) yields $\partial_x\hat{\varphi}(x,t)\big]_{x_0^-}^{x_0^+}=\chi_s\partial_t^2\hat{\varphi}(x_0,t)+\chi_s\omega_j^2\sin[\hat{\varphi}_j(t)]$, where the discontinuity in the resonator current is equal to the total current through the capacitive and Josephson branches of the transmon. Similar modification of resonator dynamics has been pointed out before for JJ-based qubits [9, 22, 25].

Equation 3 can be solved in the Fourier domain, where $\hat{\tilde{\varphi}}(x,\omega)=\int_{-\infty}^{\infty}dt\,\hat{\varphi}(x,t)e^{-i\omega t}$ can be expanded in the basis $\tilde{\varphi}_n(x,\omega)$ that solves the generalized eigenvalue problem $\left[\partial_x^2+\chi(x,x_0)\,\omega^2\right]\tilde{\varphi}_n(x,\omega)=0$, subject to continuity conditions at the ends of the resonator, i.e. $\partial_x\tilde{\varphi}_n(1^-,\omega)=\chi_R\omega^2[\tilde{\varphi}_n(1^-,\omega)-\tilde{\varphi}_n(1^+,\omega)]$ and $\partial_x\tilde{\varphi}_n(0^+,\omega)=\chi_L\omega^2[\tilde{\varphi}_n(0^-,\omega)-\tilde{\varphi}_n(0^+,\omega)]$, which models the coupling to the waveguides and associated loss. The Dirac δ-function in $\chi(x,x_0)$ leads to the discontinuity

$$-\partial_x\tilde{\varphi}_n(x)\big]_{x_0^-}^{x_0^+}=\chi_s\omega_n^2\tilde{\varphi}_n(x_0), \tag{4}$$

resulting in a modified current-conserving (CC) basis [22]. These modifications in the spectrum of the trans-

mission line resonator impact the qubit dynamics that is driven by resonator fluctuations.

The role of modal modification in Eq. (4) can be illustrated with a phenomenological model. Previously, the Purcell rate and the Lamb shift have been calculated using the Lindblad formalism in the dispersive limit [10]. An effective multimode JC model

$$\hat{\mathcal{H}}_{\rm JC} = \frac{\omega_j}{2}\hat{\sigma}_z + \sum_n \nu_n \hat{a}_n^\dagger \hat{a}_n + \sum_n g_n \left(\hat{\sigma}^+ \hat{a}_n + \hat{\sigma}^- \hat{a}_n^\dagger\right) \quad (5)$$

can be obtained from our first principles model [12], which incorporates the modifications to the resonator modes and the qubit dynamics. Resonator losses are included through a Bloch–Redfield equivalent zero-temperature master equation for the reduced density matrix of the resonator and qubit $\dot{\hat{\rho}} = -i[\hat{\mathcal{H}}_{\rm JC}, \hat{\rho}] + \frac{\kappa_n}{2}\left(2\hat{a}_n\hat{\rho}\hat{a}_n^\dagger - \{\hat{\rho}, \hat{a}_n^\dagger\hat{a}_n\}\right)$. The expressions of cavity frequencies ν_n, associated losses κ_n and modal interaction strengths g_n are given in the Supplementary Material [12]. All these quantities are functions of χ_s, the strength of the modification of the capacitance per unit length. In particular, the light-matter coupling is found as $g_n = \frac{1}{2}\gamma\sqrt{\chi_j}\sqrt{\omega_j\nu_n}\tilde{\varphi}_n(x_0)$. We show in Fig. 2a that g_n is non-monotonic [22] for any $\chi_s \neq 0$, first increasing, then turning over at a critical χ_s-dependent mode n, decreasing as $g_n \sim 1/\sqrt{n}$ in the large-n limit [12]. This high frequency behavior of g_n renders the multimode Purcell rate finite, without an imposed cutoff [26].

This phenomenon is not specific to the resonator geometry in Fig. 1a. The underlying physics is the conservation of current at the position x_0 of the qubit. At high frequency, the series capacitance χ_s becomes a short-circuit to ground, acting as a low-pass filter and suppressing mode amplitude at x_0. This is the cause of the power law drop of g_n as $n \to \infty$ (Fig. 2a). Moreover, eliminating the continuum degrees of freedom of the waveguides gives an effective decay rate for each mode, κ_n, which increases monotonically as $\kappa_n \sim n^{0.3}$ (Fig. 2b). In the Supplementary Material, we show that for $\chi_s = 0$ the resulting series Eq. (1) diverges [12], as pointed out in previous studies [8, 11]. For *any* nonzero χ_s, individual terms in the sum (1) display a universal power law $\sim n^{-2.7}$ (Fig. 2c), which guarantees convergence [27].

Solution of the Heisenberg-Langevin equations. Although we showed that the expression (1) for the Purcell decay rate converges, it is only valid in the dispersive regime $g_n \ll \delta_n$. This estimate for the Purcell decay rate and the Lamb shift will deviate substantially from the exact result for a range of order g_n around each cavity resonance, diverging as the qubit frequency approaches the resonance (see Fig. 3). This fictitious divergence can in principle be cured by solving the full multimode Master equation. Even if computational challenges relating to the long-time dynamics in such a large Hilbert space can be addressed, the resulting rate would still be subject to the TLA, RWA, Born and Markov approximations, casting a priori an uncertainty on its reliability.

An improved analytic result that is uniformly valid

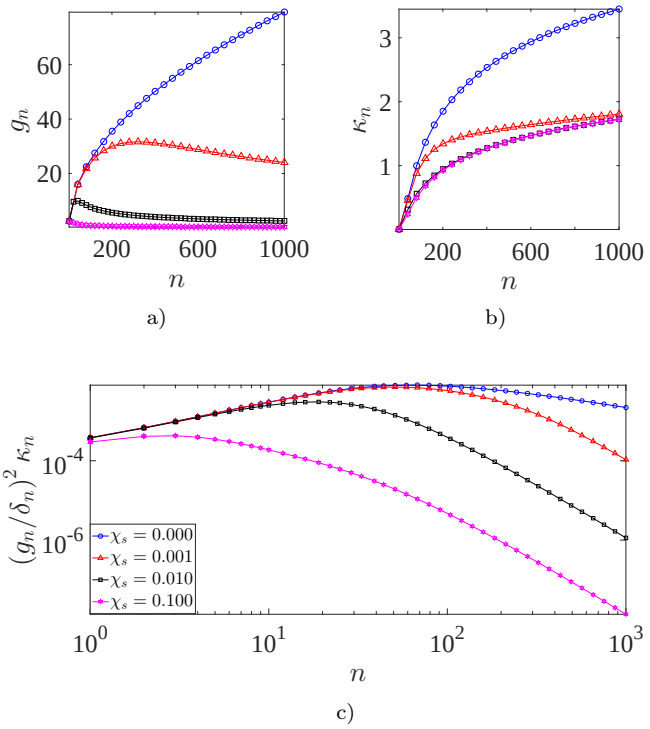

FIG. 2. (Color online) Dependence of a) coupling strength g_n, b) resonator decay rate κ_n (See [12] for derivation) and c) Purcell decay rate in the dispersive regime $(g_n/\delta_n)^2\kappa_n$ on mode number n for different values of $\chi_s = \{0, 10^{-3}, 10^{-2}, 10^{-1}\}$. Other parameters are set as $\chi_R = \chi_L = 10^{-3}$ and $x_0 = 0^+$.

in the transmon frequency, and is not limited by the aforementioned approximations can be found by solving Eqs. (2-3) perturbatively in the transmon's weak nonlinearity. EM degrees of freedom can be integrated out by solving Eq. (3) exactly, plugging into Eq. (2) and tracing over the photonic Hilbert space. To lowest order in the transmon nonlinearity $\epsilon = (E_c/E_j)^{1/2}$, where E_c and E_j are the charging and Josephson energy, respectively, the effective equation for the qubit is [24]

$$\begin{aligned}\ddot{\hat{X}}_j(t) + \omega_j^2\left[1 - \gamma + i\mathcal{K}_1(0)\right]\hat{X}_j(t) \\ = -\omega_j^2\int_0^t dt'\mathcal{K}_2(t-t')\hat{X}_j(t'),\end{aligned} \quad (6)$$

where $\hat{X}_j(t) = {\rm Tr}_{ph}\{\hat{\rho}_{ph}(0)\hat{\varphi}_j(t)\}/\phi_{\rm zpf}$ is the reduced flux operator traced over the photonic degrees of freedom and $\phi_{\rm zpf} \equiv (\sqrt{2}\epsilon)^{1/2}$ is the magnitude of the zero-point phase fluctuations. This delay equation features the memory kernels $\mathcal{K}_n(\tau) \equiv \gamma\chi_s\int_{-\infty}^{+\infty}\frac{d\omega}{2\pi}\omega^n G(x_0, x_0, \omega)e^{-i\omega\tau}$, where $G(x, x', \omega)$ is the classical EM Green's function defined by $\left[\partial_x^2 - \chi(x, x_0)\partial_t^2\right]G(x, x', \omega)e^{-i\omega t} = e^{-i\omega t}\delta(x - x')$ implying that $G(x, x', \omega)$ is the amplitude of the flux field created at x by a transmon oscillating with a frequency ω at x' [24]. The term on the right hand side of 6 is therefore proportional to the fluctuating current driving the qubit at time t, that was excited by itself at an

earlier time t'. This Green's function correctly encodes the modification of the capacitance per length. Equation (6) can be solved exactly in the Laplace domain

$$\hat{\tilde{X}}_j(s) = \frac{s\hat{X}_j(0) + \hat{\dot{X}}_j(0)}{D_j(s)}, \tag{7}$$

where $\tilde{h}(s) \equiv \int_0^\infty dt\, h(t)\, e^{-st}$, with $D_j(s)$ defined as [24]

$$D_j(s) \equiv s^2 + \omega_j^2 \left[1 - \gamma + i\mathcal{K}_1(0) + \tilde{\mathcal{K}}_2(s)\right]. \tag{8}$$

We express the characteristic function $D_j(s)$ in meromorphic form

$$D_j(s) = (s - p_j)(s - p_j^*) \prod_m \frac{(s - p_m)(s - p_m^*)}{(s - z_m)(s - z_m^*)}. \tag{9}$$

The poles of $1/D_j(s)$ are the hybridized qubit-like and resonator-like complex-valued excitation frequencies, $p_j \equiv -\alpha_j - i\beta_j$ and $p_n \equiv -\alpha_n - i\beta_n$, respectively, of the qubit-resonator system, while its zeroes $z_n \equiv -i\omega_n = -\kappa_n - i\nu_n$ correspond to bare non-Hermitian [12] cavity resonances. The real part of the qubit-like pole, α_j, is the Purcell loss rate, while $\beta_j - \omega_j$ is the Lamb shift, as shown in Fig. 1b. In the Supplementary Material, we show that $D_j(s)$ is convergent, and hence so are all hybridized frequencies, for any nonzero χ_s.

The A^2-term kept in our calculation to enforce gauge invariance plays the role of the "counterterm" discussed by Caldeira and Leggett to cancel infinite frequency renormalization [28, 29]. This problem has also been discussed in the context of the quantum theory of laser radiation [30].

Perturbative corrections. The transmon nonlinearity neglected in Eq. (6) can be reintroduced as a weak perturbation. The leading order correction to the hybridized resonances amounts to self- and cross-Kerr interactions [9, 25]. Using multi-scale perturbation theory [24, 32], the correction to the transmon qubit-like resonance β_j is given by

$$\hat{\beta}_j = \beta_j - \frac{\sqrt{2}\epsilon}{4}\omega_j \left[u_j^4 \hat{\mathcal{H}}_j(0) + \sum_n 2u_j^2 u_n^2 \hat{\mathcal{H}}_n(0)\right] \tag{10}$$

where the coefficients $u_{j,n}$ define the transformation from the hybridized to the unhybridized modes and $\hat{\mathcal{H}}_{j,n}(0)$ are the free Hamiltonians of the transmon and mode n, respectively. For $\chi_g \to 0$, we find $u_j \to 1$, $u_n = 0$ and $\beta_j \to \omega_j$ such that we recover the frequency correction of free quantum Duffing oscillator $\hat{\tilde{\omega}}_j = \omega_j[1 - \frac{\sqrt{2}\epsilon}{4}\hat{\mathcal{H}}_j(0)]$ [33]. We note three features of this result. Firstly, the correction is an operator and that expresses the fact that transmon levels are anharmonic. The anharmonicity can be calculated from the expectation value of a corrected quadrature operator [12]. Secondly, by virtue of the lowest order result being convergent without a cutoff, the perturbative corrections are also convergent in the number of modes included. Finally, this result is not limited by the qubit-resonator coupling strength or the openness of the cavity. The final result is finite for all qubit frequencies, as opposed to the dispersive-limit result. The correction to the Purcell decay is higher order and forms the subject of future work.

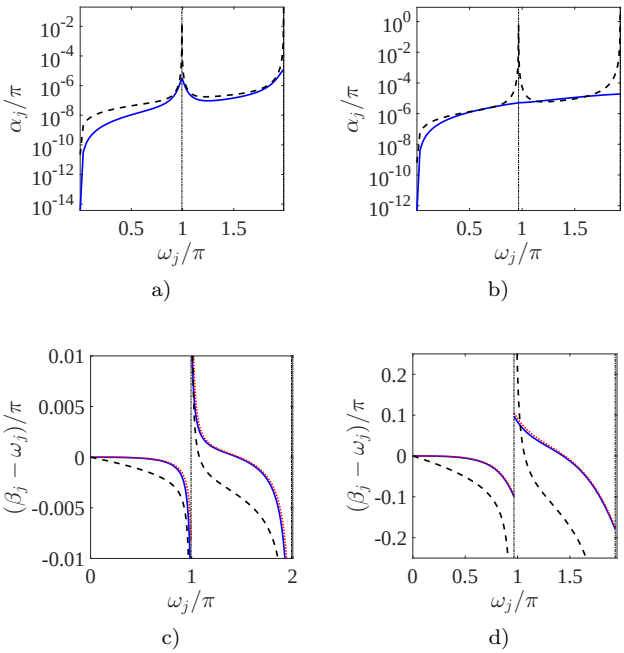

FIG. 3. (Color online) Comparison of a,b) spontaneous decay rate between the linear theory (blue solid) and the dispersive limit result γ_P (black dashed) as a function of ω_j. c,d) Lamb shift between the linear theory (blue solid), leading order perturbation (red dotted) and the dispersive limit result Δ_L (black dashed). a,c) $\chi_g = 0.001$ and b,d) $\chi_g = 0.1$. Both values of χ_g are in strong coupling regime, i.e. $g_1/\alpha_j \gg 1$. However, $\chi_g = 0.1$ ($g_1/\nu_1 = 0.1033$) reaches ultrastrong coupling [31], where multimode effects are non-negligible. The nonlinearity is set as $\epsilon = 0.1$, while other parameters are $\chi_R = \chi_L = 10^{-3}$ and $\chi_j = 0.05$. The vertical dash-dotted black line shows the position of the fundamental frequency of the resonator.

We compared the spontaneous decay from the linear theory (blue solid) to the dispersive limit estimate γ_P in Eq. (1) (black dashed) as the transmon frequency is tuned across the fundamental mode in Figs. 3a-3b. First, the spontaneous decay is asymmetric, since there are (in)finitely many modes with frequency (larger) smaller than ω_j. This feature is captured by both theories. Second, the spontaneous decay is enhanced as the qubit frequency approaches the fundamental resonator frequency. However, the dispersive limit estimate is perturbative in g_n/δ_n and hence yields a divergent result (fake kink) on resonance regardless of coupling constant, contrary to our result 9 which predicts a finite value even at ultrastrong coupling (Fig. 3b and caption).

In Figs. 3c-3d we compare the Lamb shift from the linear theory (blue solid) and the leading order pertur-

bation theory (red dotted) to the dispersive multimode estimate (black dashed) $\sum_n g_n^2/\delta_n$ [10]. Below the fundamental mode, the Lamb shift is negative due to the collective influence of all higher modes that redshifts the qubit frequency. Above the fundamental mode, there appears a competition between the hybridization with the fundamental mode and all higher modes. Close enough to the fundamental mode, the Lamb shift is positive until it changes sign, as predicted by all three curves.

Conclusion. We have presented a framework to calculate the spontaneous decay and the Lamb shift of a transmon qubit, convergent in the number of resonator modes without the need for rotating-wave, two-level, Born or Markov approximations, or a high frequency cutoff. This is achieved by an *ab initio* treatment of the quantum circuit equations of motion containing the A^2-term to enforce gauge invariance. Therefore, the modes of the resonator are modified such that the light-matter coupling is suppressed at high frequencies. Formulating the cavity resonances in terms of non-Hermitian modes provides access to the spontaneous decay, the Lamb shift, and any other QED observables in a unified way.

Acknowledgements. We acknowledge helpful discussions with Zlatko Minev and Steven Girvin. This work was supported by the U.S. Army Research Office (ARO) under Grant No. W911NF-15-1-0299.

Note. While finishing this manuscript we became aware of Ref. 34, which arrives at a similar conclusion for the Lamb shift in the dispersive regime through a different approach.

[1] D. Kleppner, Phys. Rev. Lett. **47**, 233 (1981).
[2] P. Goy, J. M. Raimond, M. Gross, and S. Haroche, Phys. Rev. Lett. **50**, 1903 (1983).
[3] R. G. Hulet, E. S. Hilfer, and D. Kleppner, Phys. Rev. Lett. **55**, 2137 (1985).
[4] W. Jhe, A. Anderson, E. A. Hinds, D. Meschede, L. Moi, and S. Haroche, Phys. Rev. Lett. **58**, 666 (1987).
[5] E. M. Purcell, H. C. Torrey, and R. V. Pound, Phys. Rev. **69**, 37 (1946).
[6] W. E. Lamb Jr and R. C. Retherford, Physical Review **72**, 241 (1947).
[7] A. Fragner, M. Göppl, J. Fink, M. Baur, R. Bianchetti, P. Leek, A. Blais, and A. Wallraff, Science **322**, 1357 (2008).
[8] A. A. Houck, J. A. Schreier, B. R. Johnson, J. M. Chow, J. Koch, J. M. Gambetta, D. I. Schuster, L. Frunzio, M. H. Devoret, S. M. Girvin, and R. J. Schoelkopf, Phys. Rev. Lett. **101**, 080502 (2008).
[9] S. E. Nigg, H. Paik, B. Vlastakis, G. Kirchmair, S. Shankar, L. Frunzio, M. H. Devoret, R. J. Schoelkopf, and S. M. Girvin, Phys. Rev. Lett. **108**, 240502 (2012).
[10] M. Boissonneault, J. M. Gambetta, and A. Blais, Phys. Rev. A **79**, 013819 (2009).
[11] S. Filipp, M. Göppl, J. M. Fink, M. Baur, R. Bianchetti, L. Steffen, and A. Wallraff, Phys. Rev. A **83**, 063827 (2011).
[12] M. Malekakhlagh, A. Petrescu, and H. E. Tureci, *Supplementary Material*.
[13] V. Weisskopf and E. Wigner, Zeitschrift für Physik A Hadrons and Nuclei **63**, 54 (1930).
[14] M. O. Scully and M. S. Zubairy, *"Quantum Optics"* (Cambridge University Press, 1997).
[15] D. O. Krimer, M. Liertzer, S. Rotter, and H. E. Türeci, Phys. Rev. A **89**, 033820 (2014).
[16] M. H. Devoret, in *Les Houches, Session LXIII*, Vol. 7, edited by S. Reynaud, E. Giacobino, and J. Zinn-Justin (Elsevier Science, 1997) pp. 351–386.
[17] W. E. Lamb, R. R. Schlicher, and M. O. Scully, Phys. Rev. A **36**, 2763 (1987).
[18] J. Koch, T. M. Yu, J. Gambetta, A. A. Houck, D. I. Schuster, J. Majer, A. Blais, M. H. Devoret, S. M. Girvin, and R. J. Schoelkopf, Phys. Rev. A **76**, 042319 (2007).
[19] J. Schreier, A. A. Houck, J. Koch, D. I. Schuster, B. Johnson, J. Chow, J. M. Gambetta, J. Majer, L. Frunzio, M. H. Devoret, *et al.*, Physical Review B **77**, 180502 (2008).
[20] M. Devoret, B. Huard, R. Schoelkopf, and L. F. Cugliandolo, eds., *"Quantum Machines: Measurement and Control of Engineered Quantum Systems: Lecture Notes of the Les Houches Summer School: Volume 96, July 2011"* (Lecture Notes of the Les Houches Summer School 96, 2014).
[21] See also the Supplementary Material for a detailed derivation of the main results of this paper, which includes Refs. [10, 14, 20, 22, 24, 35–41].
[22] M. Malekakhlagh and H. E. Türeci, Phys. Rev. A **93**, 012120 (2016).
[23] P. W. Milonni, *"The quantum vacuum: an introduction to quantum electrodynamics"* (Academic press, 2013) Chap. 3.
[24] M. Malekakhlagh, A. Petrescu, and H. E. Türeci, Phys. Rev. A **94**, 063848 (2016).
[25] J. Bourassa, F. Beaudoin, J. M. Gambetta, and A. Blais, Phys. Rev. A **86**, 013814 (2012).
[26] We note that this result is valid in the dispersive limit i.e. away from cavity resonances. In that limit, we expect this result to be fairly accurate when compared to the rate extracted from the exact time evolution of the Master equation for the multimode JC model.
[27] The power law dependence of κ_n and g_n, though universal with respect to χ_s, are specific to the chosen circuit topology.
[28] A. Caldeira and A. Leggett, Annals of Physics **149**, 374 (1983).
[29] A. J. Leggett, Phys. Rev. B **30**, 1208 (1984).
[30] F. Schwabl and W. Thirring, "Quantum theory of laser radiation," in *Ergebnisse der exakten Naturwissenschaften* (Springer Berlin Heidelberg, Berlin, Heidelberg, 1964) pp. 219–242.
[31] T. Niemczyk, F. Deppe, H. Huebl, E. P. Menzel, F. Hocke, M. J. Schwarz, J. García-Ripoll, D. Zueco, T. Hmmer, E. Solano, A. Marx, and R. Gross, Nature Physics **6**, 772 (2010).
[32] C. M. Bender and S. A. Orszag, *"Advanced mathematical methods for scientists and engineers"* (Springer Science & Business Media, 1999).

[33] C. M. Bender and L. M. A. Bettencourt, Phys. Rev. Lett. **77**, 4114 (1996).
[34] M. F. Gely, A. Parra-Rodriguez, D. Bothner, Y. M. Blanter, S. J. Bosman, E. Solano, and G. A. Steele, Phys. Rev. B **95**, 245115 (2017).
[35] L. S. Bishop, arXiv:1007.3520 [cond-mat, physics:quant-ph] (2010).
[36] A. A. Clerk, M. H. Devoret, S. M. Girvin, F. Marquardt, and R. J. Schoelkopf, Rev. Mod. Phys. **82**, 1155 (2010).
[37] P. Morse and H. Feshbach, *"Methods of theoretical physics"* (McGraw-Hill, 1953).
[38] E. N. Economou, *"Green's functions in quantum physics"*, Vol. 3 (Springer, 1984).
[39] S. Hassani, *"Mathematical physics: a modern introduction to its foundations"* (Springer Science & Business Media, 2013).
[40] H. E. Türeci, A. D. Stone, and B. Collier, Phys. Rev. A **74**, 043822 (2006).
[41] I. R. Senitzky, Phys. Rev. **119**, 670 (1960).